A Comparative Study of All-Accelerometer Strapdowns for UAV INS

Philippe Cardou (pcardou@cim.mcgill.ca)
Jorge Angeles (angeles@cim.mcgill.ca)

Department of Mechanical Engineering &
Centre for Intelligent Machines
McGill University
817 Sherbrooke St. West
Montreal, QC H3A 2K6

ABSTRACT

We analyze the possibility of using arrays of accelerometers as Inertial Navigation Systems (INS) for Unmanned Aerial Vehicles (UAV). Benefiting from the fabrication processes of MEMS technologies, accelerometers now offer several advantages over gyroscopes, such as low weight, compactness, high reliability and low cost, for example. An algorithm is introduced which allows the computation of the angular acceleration and the angular velocity of a UAV from measurements of n uniaxial accelerometers located at n arbitrary points on the UAV. By uniaxial accelerometer we mean a sensor that allows the measurement of only one point-acceleration component. It is shown that the necessary conditions for the algorithm to work are that n be greater than or equal to nine, that the points be non-collinear, and that the vectors pointing in the sensitive directions of all the sensors span the whole 3D space. Notice that such analyses have been performed before, but only for specific strapdowns and never for a completely general case, in which the positions and the orientations of the sensors are arbitrary, except for the conditions stated above. In the linear algebraic system of $3n$ equations in $2n + 9$ unknowns that has to be solved to compute the angular acceleration and the angular velocity, the coefficients of the unknowns depend only on the geometry of the accelerometer strapdown, and not on the measurements. Therefore, the condition number of the algebraic linear system gives an upper bound of the error amplification incurred when solving the linear system for any accelerometer measurements, which makes the condition number a suitable performance index for the design of UAV accelerometer strapdowns. With regard to this new performance index, a comparison of the accuracies of existing accelerometer strapdowns is conducted. Moreover, an error analysis is provided, taking into account stochastic errors—noise—and deterministic errors—bias—in the sensor outputs. Results of numerical simulations are included to validate the error models and to assess the real-time capabilities of the algorithm. Finally, a comparison between the performances of all-accelerometer strapdowns and the traditional gyroscope-accelerometer INS is reported.

1 INTRODUCTION

New operation requirements call for small, low-cost UAVs for high-risk recognition missions. As an example, the *Dragon Eye*, which is shown in Fig. 1, is meant to perform "over-the-hill" reconnaissance missions for ground personnel. Because these UAVs are to become widely used, their unit price needs to be kept very low. As their structure and propellers are relatively simple, a significant part of the price of such UAVs comes from their Inertial Navigation System (INS). Within the INS, gyroscopes are the limiting factor regarding cost and accuracy (Zorn, 2002). Indeed, the price for fiber optic angular-rate sensors is in the order of thousands of euros, whereas it is in the order of ten euros for an accelerometer. There also exist mechanical gyroscopes for which the price is more reasonable—a few tens of euros. However, these devices show very poor accuracy—typically 100 times less than

Cardou, P.; Angeles, J. (2005) A Comparative Study of All-Accelerometer Strapdowns for UAV INS. In *Advanced Sensor Payloads for UAV* (pp. 9-1 – 9-16). Meeting Proceedings RTO-MP-SET-092, Paper 9. Neuilly-sur-Seine, France: RTO. Available from: http://www.rto.nato.int/abstracts.asp.

Report Documentation Page

Form Approved
OMB No. 0704-0188

Public reporting burden for the collection of information is estimated to average 1 hour per response, including the time for reviewing instructions, searching existing data sources, gathering and maintaining the data needed, and completing and reviewing the collection of information. Send comments regarding this burden estimate or any other aspect of this collection of information, including suggestions for reducing this burden, to Washington Headquarters Services, Directorate for Information Operations and Reports, 1215 Jefferson Davis Highway, Suite 1204, Arlington VA 22202-4302. Respondents should be aware that notwithstanding any other provision of law, no person shall be subject to a penalty for failing to comply with a collection of information if it does not display a currently valid OMB control number.

1. REPORT DATE	2. REPORT TYPE	3. DATES COVERED
01 MAY 2005	**N/A**	**-**

4. TITLE AND SUBTITLE	5a. CONTRACT NUMBER
A Comparative Study of All-Accelerometer Strapdowns for UAV INS	5b. GRANT NUMBER
	5c. PROGRAM ELEMENT NUMBER
6. AUTHOR(S)	5d. PROJECT NUMBER
	5e. TASK NUMBER
	5f. WORK UNIT NUMBER
7. PERFORMING ORGANIZATION NAME(S) AND ADDRESS(ES) **Department of Mechanical Engineering & Centre for Intelligent Machines McGill University 817 Sherbrooke St. West Montreal, QC H3A 2K6**	8. PERFORMING ORGANIZATION REPORT NUMBER
9. SPONSORING/MONITORING AGENCY NAME(S) AND ADDRESS(ES)	10. SPONSOR/MONITOR'S ACRONYM(S)
	11. SPONSOR/MONITOR'S REPORT NUMBER(S)

12. DISTRIBUTION/AVAILABILITY STATEMENT
Approved for public release, distribution unlimited

13. SUPPLEMENTARY NOTES
See also ADM202032., The original document contains color images.

14. ABSTRACT

15. SUBJECT TERMS

16. SECURITY CLASSIFICATION OF:			17. LIMITATION OF ABSTRACT	18. NUMBER OF PAGES	19a. NAME OF RESPONSIBLE PERSON
a. REPORT	b. ABSTRACT	c. THIS PAGE			
unclassified	**unclassified**	**unclassified**	**UU**	**16**	

Figure 1: The *Dragon Eye*, by *AeroVironment Inc.*

their optical counterparts—and tend to be unreliable because they require a spinning top. Moreover, gyroscopes are in general bulkier and more power-demanding than accelerometers, which calls for larger battery packs. As a small UAV such as the *Dragon Eye* is to be backpack portable and launched by hand or by means of a simple bungee rope, weight is an important issue.

From all these problems comes naturally the idea of replacing all gyroscopes by an array of accelerometers that are to measure acceleration components of a constellation of points on the vehicle. If the vehicle is regarded as a rigid body, knowing the accelerations of several landmark points allows one to find the kinematic variables of the vehicle, that is, its angular acceleration $\dot{\boldsymbol{\omega}}$, its angular velocity $\boldsymbol{\omega}$, its attitude, which we will represent here by a four-dimensional array of Euler-Rodrigue parameters $\boldsymbol{\eta}$, its point-acceleration $\ddot{\mathbf{p}}$, its velocity $\dot{\mathbf{p}}$ and its position $\mathbf{p}$. This is not a new idea—see Padgaonkar et al. (1975), Mostov (2000), and Peng and Golnaraghi (2004), for example—but it has only been implemented with little success in limited applications until now. In this paper, we aim at shedding light on the lack of success of previous attempts; whether replacing gyroscopes by accelerometers is feasible, taking into account the accuracy offered by current technology. The analysis is done for a totally general case, where the vehicle is equipped with n single-axis accelerometers taken to be located at n distinct points $\{P_i\}_{i=1}^n$ and with their sensitive axes parallel to corresponding unit-vectors $\{\mathbf{q}_{i1}\}_{i=1}^n$.

2 THE ASSOCIATED ALGEBRAIC LINEAR SYSTEM

The UAV equipped with a strapdown of n accelerometers is schematized in Fig. 2. The i^{th} accelerometer is attached to point P_i of the vehicle. $\mathcal{R}$ is the inertial frame with origin $O_{\mathcal{R}}$; frame $\mathcal{V}$ is attached to the vehicle, with origin $O_{\mathcal{V}}$; and frame $\mathcal{A}_i$, $i = 1, \ldots, n$, is also attached to the rigid body, with origin P_i, and with its x-axis pointing in the positive sensing direction of the i^{th} accelerometer. Vector $\mathbf{p}$ is directed from point $O_{\mathcal{R}}$ to point $O_{\mathcal{B}}$, while $\mathbf{p}_i$ is directed from point $O_{\mathcal{R}}$ to point P_i. We also define the geometric centre C of the accelerometers $\mathbf{p}_C \equiv (1/n)\sum_{i=1}^n \mathbf{p}_i$ and $\mathbf{r}_i \equiv \mathbf{p}_i - \mathbf{p_C}$. Moreover, matrix $\mathbf{Q}$ rotates frame $\mathcal{R}$ onto frame $\mathcal{V}$, while matrix $\mathbf{Q}_i$ rotates frame $\mathcal{V}$ onto frame $\mathcal{A}_i$.

The angular acceleration $\dot{\boldsymbol{\omega}}$ and the angular velocity $\boldsymbol{\omega}$ can be computed from the equation of rigid-body motion of elementary mechanics:

$$\ddot{\mathbf{p}}_i = \ddot{\mathbf{p}}_C + \dot{\boldsymbol{\omega}} \times (\ddot{\mathbf{p}}_i - \ddot{\mathbf{p}}_C) + \boldsymbol{\omega} \times \boldsymbol{\omega} \times (\ddot{\mathbf{p}}_i - \ddot{\mathbf{p}}_C)\,. \tag{1}$$

This equation can be rewritten in the more compact form

$$\ddot{\mathbf{p}}_i - \ddot{\mathbf{p}}_C = \mathbf{W}\mathbf{r}_i, \quad i = 1, \ldots, n, \tag{2}$$

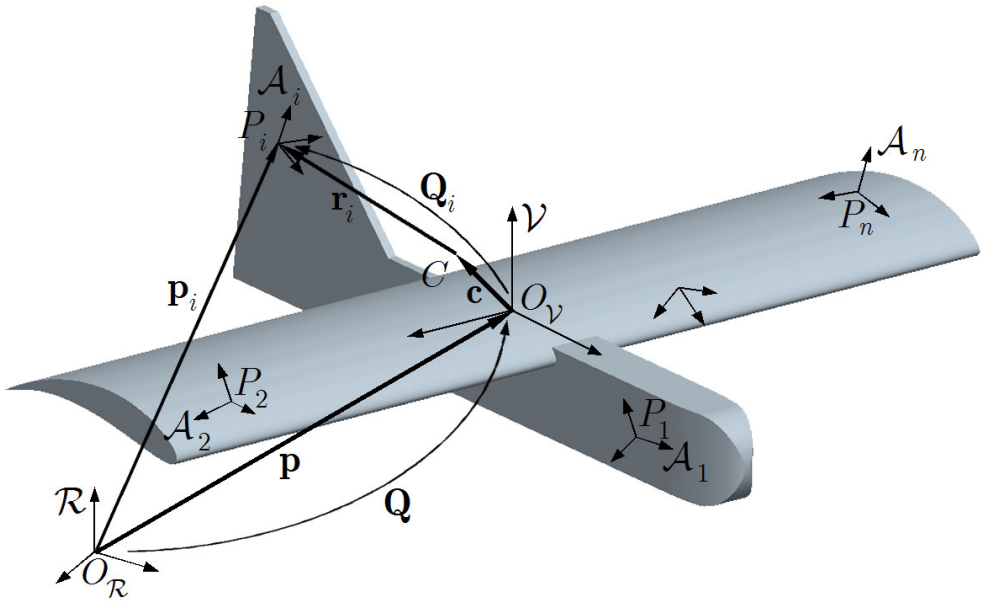

Figure 2: The *Dragon Eye* and hypothetic measurement points

where $\mathbf{W} \equiv \dot{\mathbf{\Omega}} + \mathbf{\Omega}^2$, and $\mathbf{\Omega}$ is the cross-product matrix[1] (CPM) of $\boldsymbol{\omega}$. $\mathbf{W}$ can be referred to as the angular acceleration matrix, as in Angeles (2003). Equations (2) can be rewritten as

$$\mathbf{Q}_i[\ddot{\mathbf{p}}_i]_{\mathcal{A}_i} - \frac{1}{n}\sum_{j=1}^{n}\mathbf{Q}_j[\ddot{\mathbf{p}}_j]_{\mathcal{A}_j} = \mathbf{W}\mathbf{r}_i, \quad i = 1, \ldots, n. \tag{3}$$

Let us now partition the rotation matrices into three column-vectors and define the components of $\ddot{\mathbf{p}}_i$ in their corresponding frames $\mathcal{A}_i$:

$$\mathbf{Q}_i = \begin{bmatrix}\mathbf{q}_{i1} & \mathbf{q}_{i2} & \mathbf{q}_{i3}\end{bmatrix}, \quad [\ddot{\mathbf{p}}_i]_{\mathcal{A}_i} = \begin{bmatrix}a_{i1}\\ a_{i2}\\ a_{i3}\end{bmatrix}. \tag{4}$$

As acceleration component a_{i1} is along the sensitive axis of the i^{th} accelerometer, and is hence assumed to be known, whereas the two other components remain unknown. Thus, eq. (3) becomes

$$a_{i1}\mathbf{q}_{i1} + a_{i2}\mathbf{q}_{i2} + a_{i3}\mathbf{q}_{i3} - \ddot{\mathbf{c}}_x - \frac{1}{n}\sum_{j=1}^{n}a_{j2}\mathbf{q}_{j2} - \frac{1}{n}\sum_{j=1}^{n}a_{j3}\mathbf{q}_{j3} = \mathbf{W}\mathbf{r}_i, \quad i = 1, \ldots, n, \tag{5}$$

where

$$\ddot{\mathbf{c}}_x = \frac{1}{n}\sum_{j=1}^{n}a_{j1}\mathbf{q}_{j1}.$$

With $\ddot{\mathbf{c}}_x$ defined as the centroid of all the measured components of the point-accelerations expressed in the body frame $\mathcal{B}$. We move all unknown terms of eq. (5) to the right-hand side, thus obtaining

$$\underbrace{a_{i1}\mathbf{q}_{i1} - \ddot{\mathbf{c}}_x}_{\text{known}} = \underbrace{\mathbf{W}\mathbf{r}_i - a_{i2}\mathbf{q}_{i2} - a_{i3}\mathbf{q}_{i3} + \frac{1}{n}\sum_{j=1}^{n}a_{j2}\mathbf{q}_{j2} + \frac{1}{n}\sum_{j=1}^{n}a_{j3}\mathbf{q}_{j3}}_{\text{unknown}}, \quad i = 1, \ldots, n, \tag{6}$$

[1] CPM($\mathbf{v}$) is defined as $\partial(\mathbf{v} \times \mathbf{x})/\partial\mathbf{x}$, for any $\mathbf{x} \in \mathbb{R}^3$, with $\mathbf{v} \in \mathbb{R}^3$ as well.

Further, we partition $\mathbf{W}$ into three row-vectors:

$$\mathbf{W} = \begin{bmatrix} \mathbf{w}_1^T \\ \mathbf{w}_2^T \\ \mathbf{w}_3^T \end{bmatrix} \tag{7}$$

This allows us to rewrite eq. (6) as

$$a_{i1}\mathbf{q}_{i1} - \ddot{\mathbf{c}}_x = \mathbf{R}_i\mathbf{w} - a_{i2}\mathbf{q}_{i2} - a_{i3}\mathbf{q}_{i3} + \frac{1}{n}\sum_{j=1}^{n} a_{j2}\mathbf{q}_{j2} + \frac{1}{n}\sum_{j=1}^{n} a_{j3}\mathbf{q}_{j3}, \quad i = 1, \ldots, n, \tag{8}$$

where

$$\mathbf{R}_i = \begin{bmatrix} \mathbf{r}_i^T & \mathbf{0}^T & \mathbf{0}^T \\ \mathbf{0}^T & \mathbf{r}_i^T & \mathbf{0}^T \\ \mathbf{0}^T & \mathbf{0}^T & \mathbf{r}_i^T \end{bmatrix}, \quad \text{and} \quad \mathbf{w} = \begin{bmatrix} \mathbf{w}_1 \\ \mathbf{w}_2 \\ \mathbf{w}_3 \end{bmatrix}.$$

From eq. (8), we cast the set of matrix equations into a single one:

$$\mathbf{R}\mathbf{w} + \mathbf{A}\mathbf{a} = \mathbf{b}, \tag{9}$$

where

$$\mathbf{R} = \begin{bmatrix} \mathbf{R}_1 \\ \mathbf{R}_2 \\ \vdots \\ \mathbf{R}_n \end{bmatrix},$$

$$\mathbf{A} = \begin{bmatrix} \alpha\mathbf{q}_{12} & \alpha\mathbf{q}_{13} & \beta\mathbf{q}_{22} & \beta\mathbf{q}_{23} & \cdots & \beta\mathbf{q}_{n2} & \beta\mathbf{q}_{n3} \\ \beta\mathbf{q}_{12} & \beta\mathbf{q}_{13} & \alpha\mathbf{q}_{22} & \alpha\mathbf{q}_{23} & \cdots & \beta\mathbf{q}_{n2} & \beta\mathbf{q}_{n3} \\ \vdots & \vdots & \vdots & \vdots & \ddots & \vdots & \vdots \\ \beta\mathbf{q}_{12} & \beta\mathbf{q}_{13} & \beta\mathbf{q}_{22} & \beta\mathbf{q}_{23} & \cdots & \alpha\mathbf{q}_{n2} & \alpha\mathbf{q}_{n3} \end{bmatrix}, \quad \mathbf{a} = \begin{bmatrix} a_{12} \\ a_{13} \\ a_{22} \\ a_{23} \\ \cdots \\ a_{n2} \\ a_{n3} \end{bmatrix},$$

with $\alpha \equiv (1-n)/n$, $\beta \equiv 1/n$, and

$$\mathbf{b} = \begin{bmatrix} a_{11}\mathbf{q}_{11} - \ddot{\mathbf{c}}_x \\ a_{21}\mathbf{q}_{21} - \ddot{\mathbf{c}}_x \\ \vdots \\ a_{n1}\mathbf{q}_{n1} - \ddot{\mathbf{c}}_x \end{bmatrix}.$$

Now, we rewrite the linear system of eq. (9) as

$$\mathbf{M}\mathbf{x} = \mathbf{b}, \tag{10}$$

where

$$\mathbf{M} = \begin{bmatrix} \mathbf{A} & \mathbf{R} \end{bmatrix}, \text{ and } \quad \mathbf{x} = \begin{bmatrix} \mathbf{a}^T & \mathbf{w}^T \end{bmatrix}^T. \tag{11}$$

Matrix $\mathbf{W}$ is thus found by solving the foregoing linear system of $3n$ equations in $2n + 9$ unknowns. One can notice that matrix $\mathbf{M}$ in eq. (10) depends only on the configuration of the accelerometer array and neither on the measurements nor the orientation of frame $\mathcal{V}$ with respect to frame $\mathcal{R}$. Thus, we can render this matrix in upper-triangular form off-line, by means of Householder reflections (Golub and Van Loan, 1983), thereby obtaining a system in the form

$$\mathbf{U}\mathbf{x} = \mathbf{H}^T\mathbf{b}, \tag{12}$$

where $\mathbf{U}$ is a $3m \times 2m + 9$ upper-triangular matrix, and $\mathbf{H}$ is a $3m \times 3m$ orthogonal matrix.

3 A PERFORMANCE INDEX FOR ACCELEROMETER STRAPDOWNS

3.1 The Condition Number of $\mathbf{M}$

For starters, we ascertain whether $\mathbf{M}$ is of full rank. From eq. (11), we draw the necessary conditions for the associated linear system to be either determined or overdetermined:

1. $n \geq 9$;
2. points $\{P_i\}_{i=1}^n$ are non-collinear;
3. vectors $\{\mathbf{q}_{i,1}\}_{i=1}^n$ span $\mathbb{R}^3$;
4. $\{P_i\}_{i=1}^n$ and $\{\mathbf{q}_{i,1}\}_{i=1}^n$ are chosen so that the columns of $\mathbf{A}$ and $\mathbf{R}$ are linearly independent.

As matrix $\mathbf{M}$ depends only on the geometry of the accelerometer strapdown and not on the measurements, it can be used as a performance index to compare different strapdowns. Indeed, a good geometry is one for which the error in the acceleration measurements does not amplify when solving eq. (10). The condition number $\kappa(\mathbf{M})$ gives a measure of the sensitivity of the solution of a linear system to roundoff errors, i.e.,

$$\frac{\|\delta\mathbf{x}\|}{\|\mathbf{x}\|} \leq \kappa(\mathbf{M}) \left(\frac{\|\delta\mathbf{M}\|}{\|\mathbf{M}\|} + \frac{\|\delta\mathbf{b}\|}{\|\mathbf{b}\|} \right),$$

where $\delta\mathbf{x}$, $\delta\mathbf{M}$ and $\delta\mathbf{b}$ are the errors on $\mathbf{x}$, $\mathbf{M}$ and $\mathbf{b}$, respectively. However, $\kappa(\mathbf{M})$ cannot be computed directly here, as matrix $\mathbf{M}$ is dimensionally non-homogeneous. We normalize this matrix using the concept of characteristic length:

$$\overline{\mathbf{M}} \equiv \begin{bmatrix} \mathbf{A} & (1/l)\mathbf{R} \end{bmatrix}, \tag{13}$$

where l is the characteristic length of the accelerometer strapdown, and is defined as the normalizing length l resulting in the lowest condition number of $\mathbf{A}$ augmented with nondimensionalized $\mathbf{R}$. Hence, we can write:

$$\kappa(\overline{\mathbf{M}}) = \min_l(\kappa(\begin{bmatrix} \mathbf{A} & (1/l)\mathbf{R} \end{bmatrix})). \tag{14}$$

Here, we will use the Frobenius norm, which can be defined, for any matrix $\mathbf{B} \in \mathbb{R}^{m\times p}$ with $m \geq p$, as:

$$\|\mathbf{B}\|_F \equiv \sqrt{\frac{1}{p}\mathrm{tr}\,(\mathbf{B}^T\mathbf{B})} = \sqrt{\frac{1}{p}\mathrm{tr}\,(\mathbf{B}\mathbf{B}^T)} \tag{15}$$

Let us also define the orthogonal projectors $\mathbf{P}_r$ and $\mathbf{P}_a$ of matrices $\mathbf{R}$ and $\mathbf{A}$, respectively:

$$\mathbf{P}_r \equiv \mathbf{1}_{3n\times 3n} - \mathbf{R}(\mathbf{R}^T\mathbf{R})^{-1}\mathbf{R}^T; \tag{16}$$

$$\mathbf{P}_a \equiv \mathbf{1}_{3n\times 3n} - \mathbf{A}(\mathbf{A}^T\mathbf{A})^{-1}\mathbf{A}^T; \tag{17}$$

where $\mathbf{1}_{3n\times 3n}$ is the $3n \times 3n$ identity matrix. Using the Frobenius norm allows us to obtain symbolic expressions for the characteristic length and the associated condition number, namely,

$$l = \sqrt[4]{\frac{\alpha\delta}{\beta\gamma}}, \text{ and } \kappa_F(\overline{\mathbf{M}}) = \frac{1}{2n+9}\left(\sqrt{\alpha\gamma} + \sqrt{\beta\delta}\right) \tag{18}$$

where $\alpha \equiv 3\sum_{i=1}^n \|\mathbf{r}_i\|^2$, $\beta \equiv 2n-2$, $\gamma \equiv \mathrm{tr}[(\mathbf{R}^T\mathbf{P}_a\mathbf{R})^{-1}]$, and $\delta \equiv \mathrm{tr}[(\mathbf{A}^T\mathbf{P}_r\mathbf{A})^{-1}]$.

The proof of these relations is not included here due to space limitations, but is available upon request.

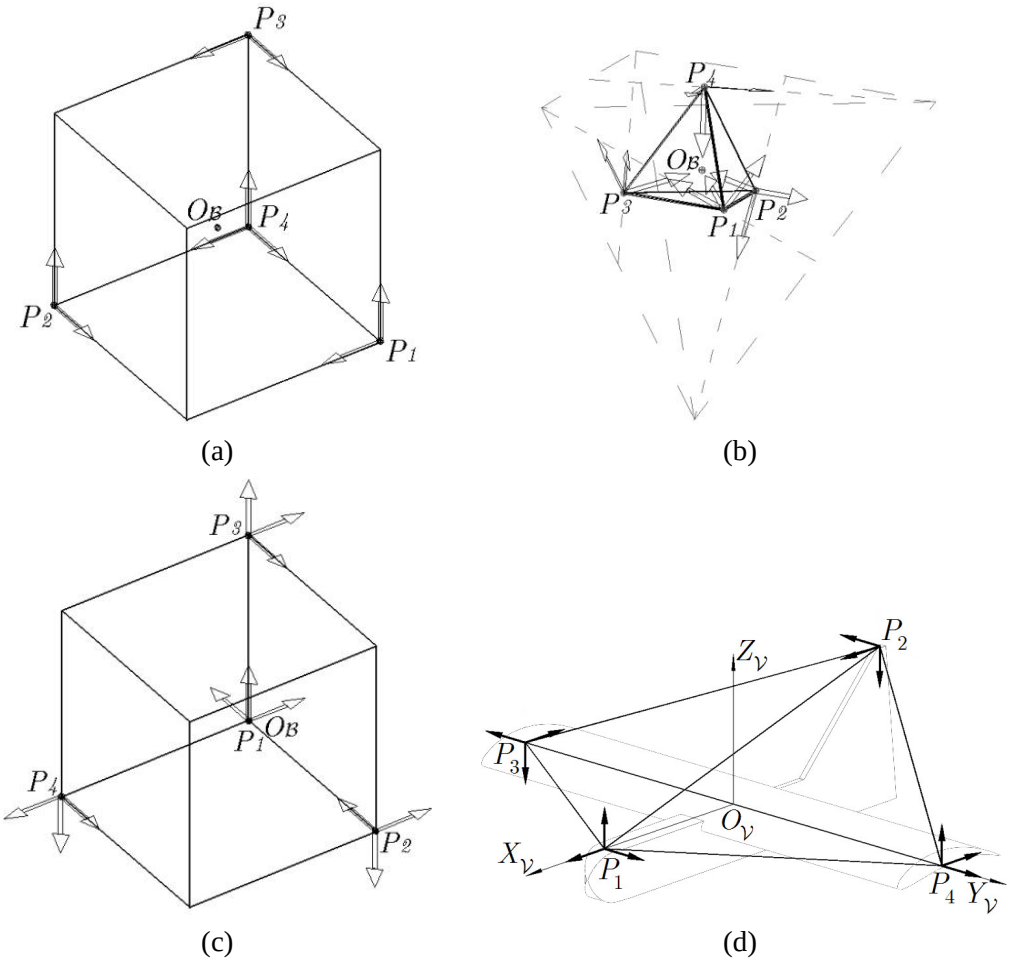

Figure 3: A sample of accelerometer strapdowns (a) nine accelerometers (Padgaonkar et al., 1975); (b) a tetrahedron-shaped strapdown of twelve accelerometers, *Plato* (Parsa et al., 2003b); (c) twelve accelerometers (Peng and Golnaraghi, 2004); and (d) proposed strapdown of twelve accelerometers for a UAV

3.2 Examples

Using this new performance criterion, we can evaluate the efficiency of some accelerometer strapdowns which have been proposed before. A sample is shown in Fig. 3, along with a new possible strapdown geometry for a UAV. We obtain the condition-number values of Table 1 for the shapes depicted in Fig. 3, where $\kappa_F(\overline{\mathbf{M}})$ is the Frobenius-norm condition number and $\kappa_2(\overline{\mathbf{M}})$ is the 2-norm condition number. The edges of the Platonic solids are all taken to be 100 mm long. In the case of the UAV-strapdown, the coordinates of points $\{P_i\}_{i=1}^4$ in frame $\mathcal{V}$ are

$$[\mathbf{p}_1]_\mathcal{V} = \begin{bmatrix} 0.5 \\ 0 \\ 0 \end{bmatrix} \text{ m, } [\mathbf{p}_2]_\mathcal{V} = \begin{bmatrix} -0.5 \\ 0 \\ 0.25 \end{bmatrix} \text{ m, } [\mathbf{p}_3]_\mathcal{V} = \begin{bmatrix} 0 \\ -0.5 \\ 0 \end{bmatrix} \text{ m, and } [\mathbf{p}_4]_\mathcal{V} = \begin{bmatrix} 0 \\ 0.5 \\ 0 \end{bmatrix} \text{ m.} \tag{19}$$

Table 1: Properties of accelerometer arrays

accelerometer array	l	$\kappa_F(\overline{\mathbf{M}})$	$\kappa_2(\overline{\mathbf{M}})$
Padgaonkar et al. (1975)	135.3 mm	2.50	9.76
Parsa et al. (2003b)	113.1 mm	1.46	3.16
Peng and Golnaraghi (2004)	164.2 mm	1.35	3.15
UAV strapdown	555.4 mm	2.35	11.66

One can see that the condition numbers for the strapdown of Peng and Golnaraghi (2004) and for *Plato* are fairly low, although they are above their lower bound of unity. As the shape of the UAV constrains the geometry, the resulting strapdown is further from the shape of a Platonic array, and, therefore, its condition number is higher than that of other strapdowns.

4 ERROR ANALYSIS

As the aim of this paper is to compare the accuracy of all-accelerometer strapdowns with that of angular-rate sensor strapdowns, we will limit the error analysis to the computation of the angular acceleration $\dot{\boldsymbol{\omega}}$ and the angular velocity $\boldsymbol{\omega}$.

4.1 Error on the Angular Acceleration $\dot{\omega}$

The sources of error affecting the angular acceleration matrix can be classified as deterministic or stochastic. The deterministic errors are

1. the errors on the position of the accelerometers $\{\delta\mathbf{r}_i\}_{i=1}^n$;
2. the errors on the orientation of accelerometers, which can be represented by their corresponding rotation matrices $\{\delta\mathbf{Q}_i\}_{i=1}^n$;
3. the bias errors on the sensor output $\{\delta a_{i1}^b\}_{i=1}^n$;
4. the non-linearity errors and the scaling errors, which we label altogether as $\{\delta a_{i1}^s\}_{i=1}^n$.

The stochastic errors are essentially noise in the accelerometer outputs $\{\delta a_{i1}^n\}_{i=1}^n$. Notice that no knowledge of the gravity field is required to compute the angular acceleration matrix. Indeed, uniform accelerations of the UAV do not contribute to any of its rates of rotation. However, uniform acceleration does have an effect on the error in the angular acceleration matrix if there are errors on the accelerometer orientations, that is, if $\delta\mathbf{Q}_i \neq \mathbf{1}_{3\times3}$, where $\mathbf{1}_{3\times3}$ is the 3×3 identity matrix.

In our case, we will assume that the accelerometer strapdown is working under ideal conditions, that is, we assume that the accelerometer strapdown has been calibrated such that the positions and the orientations of all the sensors are accurately known. Also, the UAV is taken to be perfectly rigid, which means that the position and orientation errors remain constant throughout the flight. We also assume that the accelerometer sensitivity has been characterized and accounted for, which leaves us with the error $\delta a_{i1} = \delta a_{i1}^b + \delta a_{i1}^n$. Here, δa_{i1}^b and δa_{i1}^n will be considered as random variables with normal probability densities. This assumption is reasonable, because most sensor characteristics are close to being normally distributed—for example, see Analog Devices (2005).

Now, we can rewrite eq. (10) in *normal form*:

$$\overline{\mathbf{M}}\overline{\mathbf{x}} = \mathbf{b}, \tag{20}$$

where $\overline{\mathbf{x}} \equiv [\mathbf{a}^T \quad l\mathbf{w}^T]^T$. From previous assumptions, we can write the perturbed system of eq. (20) as

$$\overline{\mathbf{M}}\,(\overline{\mathbf{x}} + \delta\overline{\mathbf{x}}) = \mathbf{b} + \delta\mathbf{b}. \tag{21}$$

Notice that, since the only source of errors considered comes from the measurements, matrix $\overline{\mathbf{M}}$ is known accurately. We simplify the perturbed equation using eq. (20), which leads to

$$\overline{\mathbf{M}}\delta\overline{\mathbf{x}} = \delta\mathbf{b}. \tag{22}$$

As all the equations of the foregoing linear system come from rigid-body motion equations, the system is overdetermined only in its form. Therefore, the exaction solution can be obtained by finding its least-square approximation. Symbolically, this is done using the Moore-Penrose generalized inverse:

$$\delta\overline{\mathbf{x}} = \overline{\mathbf{M}}^{\dagger}\delta\mathbf{b}, \tag{23}$$

where $\overline{\mathbf{M}}^{\dagger} \equiv (\overline{\mathbf{M}}^T\overline{\mathbf{M}})^{-1}\overline{\mathbf{M}}^T$. We now take the 2-norm on both sides of the equation, which yields

$$\|\delta\overline{\mathbf{x}}\|_2 = \|\overline{\mathbf{M}}^{\dagger}\delta\mathbf{b}\|_2. \tag{24}$$

From the definition of the 2-norm, eq. (24) can be rewritten as an inequality, namely,

$$\|\delta\overline{\mathbf{x}}\|_2 \leq \|\overline{\mathbf{M}}^{\dagger}\|_2\|\delta\mathbf{b}\|_2. \tag{25}$$

Here, $\|\overline{\mathbf{M}}^{\dagger}\|_2$ depends only on the strapdown geometry. This norm can be computed as $\|\overline{\mathbf{M}}^{\dagger}\|_2 = 1/\sqrt{\lambda_{min}}$, where λ_{min} is the smallest eigenvalue of $\overline{\mathbf{M}}^T\overline{\mathbf{M}}$.

On the other hand, $\delta\mathbf{b}$ depends on the acceleration measurements. From eq. (9), we obtain

$$\delta\mathbf{b} = \begin{bmatrix} \delta a_{11}\mathbf{q}_{11} - \delta\ddot{\mathbf{c}}_x \\ \delta a_{21}\mathbf{q}_{21} - \delta\ddot{\mathbf{c}}_x \\ \vdots \\ \delta a_{n1}\mathbf{q}_{n1} - \delta\ddot{\mathbf{c}}_x \end{bmatrix}. \tag{26}$$

Hence, the 2-norm of $\delta\mathbf{b}$ becomes

$$\|\delta\mathbf{b}\|_2^2 = \delta\mathbf{b}^T\delta\mathbf{b} = \sum_{i=1}^{n}(\delta a_{i1})^2 - 2\delta\ddot{\mathbf{c}}_x^T\sum_{i=1}^{n}\delta a_{i1}\mathbf{q}_{i1} + n\delta\ddot{\mathbf{c}}_x^T\delta\ddot{\mathbf{c}}_x \tag{27}$$

From eq. (5), we find

$$\delta\ddot{\mathbf{c}}_x = \frac{1}{n}\sum_{j=1}^{n}\delta a_{j1}\mathbf{q}_{j1}. \tag{28}$$

Therefore, we can rewrite eq. (27) as

$$\|\delta\mathbf{b}\|_2^2 = \frac{n-1}{n}\sum_{i=1}^{n}(\delta a_{i1})^2 - \frac{1}{n}\sum_{i=1}^{n}\sum_{\substack{j=1\\ j\neq i}}^{n}\delta a_{i1}\delta a_{j1}\mathbf{q}_{i1}^T\mathbf{q}_{j1}. \tag{29}$$

We replace each measurement error δa_{i1} by its rms-value $\delta a_{rms} \equiv \sqrt{(\delta a_{rms}^b)^2 + (\delta a_{rms}^n)^2}$, where δa_{rms}^b and δa_{rms}^n are the standard deviations of the bias errors and the noise, respectively. This leads to the approximative inequality

$$\|\delta\mathbf{b}\|_2^2 \lessapprox (\delta a_{rms})^2\left(n - 1 + \frac{1}{n}\sum_{i=1}^{n}\sum_{\substack{j=1\\ j\neq i}}^{n}\left|\mathbf{q}_{i1}^T\mathbf{q}_{j1}\right|\right) \tag{30}$$

$$\lessapprox 2(n-1)(\delta a_{rms})^2. \tag{31}$$

Upon substituting the foregoing result in eq. (25), we obtain an approximative upper bound for the 2-norm of $\delta\overline{\mathbf{x}}$, namely,

$$\|\delta\overline{\mathbf{x}}\|_2 \lessapprox \sqrt{2(n-1)}\|\overline{\mathbf{M}}^{\dagger}\|_2\delta a_{rms}. \tag{32}$$

If we assume the error is evenly spread over $\overline{\mathbf{x}}$, we can compute the average error $\delta\overline{x}$ on the entries of $\overline{\mathbf{x}}$ as

$$\delta\overline{x} \lessapprox \|\delta\overline{\mathbf{x}}\|_2/\sqrt{2n+9}. \tag{33}$$

Thus, the error $\delta\overline{w}$ on the entries of $\mathbf{W}$ can be estimated as

$$\delta\overline{w} = \delta\overline{x}/l. \tag{34}$$

From the definition of $\mathbf{W}$, it is apparent that the angular acceleration $\dot{\boldsymbol{\omega}}$ can be computed from the angular acceleration matrix as

$$\dot{\boldsymbol{\omega}} = \text{vect}(\mathbf{W}) \equiv \frac{1}{2}\begin{bmatrix} w_{3,2} - w_{2,3} \\ w_{1,3} - w_{3,1} \\ w_{2,1} - w_{1,2} \end{bmatrix}, \tag{35}$$

where $w_{i,j}$ is the (i,j) entry of $\mathbf{W}$. Thus, the upper bound $\delta\dot{\overline{\omega}}$ for the error on the components of the angular acceleration becomes

$$\delta\dot{\overline{\omega}} = \delta\overline{w} \lessapprox \sqrt{\frac{2n-2}{2n+9}}\frac{\|\overline{\mathbf{M}}^{\dagger}\|_2 \delta a_{rms}}{l}. \tag{36}$$

4.2 Error on the Angular Velocity $\boldsymbol{\omega}$

Two methods have been used to compute the angular velocity in previous works. The two methods proposed are reviewed here, and corresponding error estimates are derived.

4.2.1 First Method: Integrating the Angular Acceleration

In this method—see Padgaonkar et al. (1975) and Mostov (2000), for example—the angular velocity at time t is computed as

$$\boldsymbol{\omega}(t) = \boldsymbol{\omega}(0) + \int_0^t \dot{\boldsymbol{\omega}}(\tau)d\tau. \tag{37}$$

No matter what the integration method is, we always have

$$\boldsymbol{\omega}(t) \approx \boldsymbol{\omega}(0) + \Delta t \sum_{j=1}^{k} \dot{\boldsymbol{\omega}}(j\Delta t), \tag{38}$$

where $t = k\Delta t$ and Δt is the time interval between to acceleration measurements—Δt is assumed to be constant. Thus, the error $\delta\omega$ on the angular velocity components becomes

$$\Delta\omega \approx \Delta t \sum_{j=1}^{k} \delta\dot{\overline{\omega}}(j\Delta t) \tag{39}$$

$$\lessapprox \sqrt{\frac{2n-2}{2n+9}}\frac{\|\overline{\mathbf{M}}^{\dagger}\|_2}{l}\Delta t \sum_{j=1}^{k} \delta a_{rms}. \tag{40}$$

Here, δa_{rms} was defined as a constant and, therefore, it can be taken out of the sum. Doing this yields an upper bound, which is too large. Instead, we can replace it by the random variable $\delta a_{i1}(t)$, which gives

$$\delta\omega \lessapprox \sqrt{\frac{2n-2}{2n+9}}\frac{\|\overline{\mathbf{M}}^{\dagger}\|_2}{l}\Delta t \sum_{j=1}^{k} \left(\delta a_{i1}^b + \delta a_{i1}^n(j\Delta t)\right). \tag{41}$$

Assuming that the noise component has a mean value of 0, the angular velocity error due to the bias error $\delta\omega^b$ of the right-hand side of inequation (41) is

$$\delta\omega^b = \sqrt{\frac{2n-2}{2n+9}}\frac{\|\overline{\mathbf{M}}^{\dagger}\|_2 t\delta a_{rms}^b}{l}. \tag{42}$$

Upon neglecting the variance in the bias errors of different sensors, the central limit theorem (Bendat, 1971) yields the standard deviation

$$\delta\omega^n = \sqrt{\frac{2n-2}{2n+9}}\frac{\|\overline{\mathbf{M}}^{\dagger}\|_2\sqrt{t\Delta t}\delta a^n_{rms}}{l}. \tag{43}$$

Finally, we freely add the average and the rms-value to compute the upper bound $\delta\omega$, that is,

$$\delta\omega \lessapprox \delta\omega^b + \delta\omega^n. \tag{44}$$

The error bound is found to grow linearly with time, which is natural, since time-integration is an unstable process—it has one imaginary pole. To cope with this problem, Parsa et al. (2003a) proposed to compute the angular velocity from the centripetal acceleration.

4.2.2 Second Method: Square-Rooting the Centripetal Acceleration

This method requires that an estimate $\hat{\boldsymbol{\omega}}$ of the angular velocity be computed from time-integration of the angular acceleration, namely,

$$\hat{\boldsymbol{\omega}}(t) = \boldsymbol{\omega}(t-\Delta t) + \int_{t-\Delta t}^{t} \dot{\boldsymbol{\omega}}(\tau)d\tau. \tag{45}$$

Afterwards, $\boldsymbol{\omega}(t)$ is computed as

$$\begin{aligned} & & w'_i &= w_{i,i} - \frac{1}{2}\mathrm{tr}(\mathbf{W}), \\ &\text{if } w'_i > 0 & & \\ & & \omega_i &= \mathrm{sgn}(\hat{\omega}_i)\sqrt{w_{i,i} - \frac{1}{2}\mathrm{tr}(\mathbf{W})}, \\ &\text{else} & & \\ & & \omega_i &= 0, \quad i = 1,2,3, \\ &\text{end if} & & \end{aligned}$$

where ω_i and $\hat{\omega}_i$ are the i^{th} entries of $\boldsymbol{\omega}$ and $\hat{\boldsymbol{\omega}}$, respectively. If we assume that the sign of ω_i can be determined accurately, its error $\delta\omega_i$ depends only on the diagonal entries of $\mathbf{W}$. Therefore, we can write

$$\delta\omega_i = \sum_{j=1}^{3}\frac{\partial\omega_i}{\partial w_{j,j}}\delta w_{j,j} \lessapprox \delta\overline{w}\sum_{j=1}^{3}\left|\frac{\partial\omega_i}{\partial w_{j,j}}\right| = \frac{3\delta w}{4\,|\omega_i|}. \tag{46}$$

If we have to compute one single upper-bound $\delta\omega$ to the angular velocity components, then we take the maximum of the three bounds, namely

$$\delta\omega = \max_{i=1,2,3}\delta\omega_i = \frac{3\delta w}{4\,\min_{i=1,2,3}|\omega_i|}. \tag{47}$$

This last expression does not depend on time, which is why this method seems attractive as compared to the time-integration method. However, it brings about another major problem: the error-bound blows up whenever one of the angular velocity components becomes null. Perhaps a combination of both methods is desirable, but this is out of the scope of this paper.

5 SIMULATION AND VALIDATION OF ERROR ESTIMATES

Simulations were performed in order to validate the error estimates obtained and to compare the performance of all-accelerometer strapdowns with that of gyroscopes. The simulation was carried out using the strapdown shown in Fig. 3(d). The accelerometers are taken to have a high accuracy: their bias errors δa^b_{i1} follow a normal distribution with zero mean and standard deviation of 0.1 mg, while their noise δa^n_{i1} is also distributed normally with a 1 mg rms-value.

The virtual motion is that of a UAV turning in circles around point $O_{\mathcal{R}}$, as shown in Fig. 4. As this is meant to correspond to what would happen in a typical recognition mission, we choose plausible values of speed and radius of turn, namely, $v = 15$ m/s and $\rho = 200$ m. This corresponds to a constant angular velocity $\boldsymbol{\omega} = [0 \quad 0 \quad 0.075]^T$ rad/s.

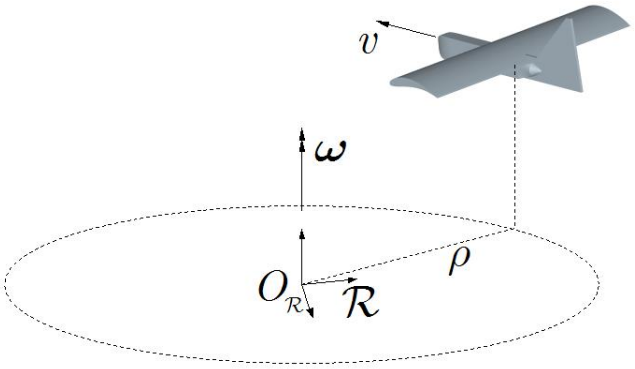

Figure 4: Sample motion

Figure 5(a) shows the resulting signals from one of the three accelerometers located at P_1, with a sampling rate of 100 Hz. The sensitive axis of this accelerometer is parallel to the pitch axis of the UAV. The components of the angular acceleration are displayed in Fig. 6(b) along with the bounds on the error on the angular acceleration components, which were computed using eq. (34). The values of $\|\overline{\mathbf{M}}^{\dagger}\|_2$ and l for the strapdown used are 4.807 and $l = 0.5554$ m, respectively, while the measurement error is taken to be $\delta a_{rms} = 1$ mg. Notice that for the prescribed motion, the real angular acceleration is null, and, therefore, the measured angular acceleration $\hat{\dot{\boldsymbol{\omega}}}$ is equal to its error $\delta\dot{\boldsymbol{\omega}}$.

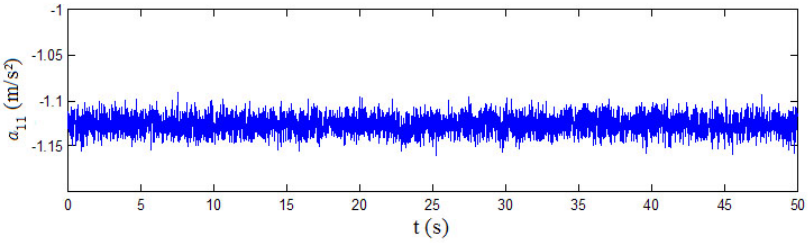

Figure 5: Signal from accelerometer #1 at point P_1

The angular velocity was computed using both the integration method and the centripetal acceleration method, leading to the results of Figs. 7 and 8. From Figs. 6 and 7, it is apparent that the error models derived for the angular acceleration and the angular velocity computed by time-integrating the angular acceleration are accurate. However, the error bound for the angular velocity computed from the centripetal acceleration is somewhat too large. A possible reason for this is that all higher-order derivatives of $\delta\omega_i$ tend to infinity as $\omega_i \to 0$. Therefore, it becomes more difficult to predict the error magnitude at low angular velocities. Nevertheless, the estimated error bound is of the same orders of magnitude as the simulated error, and, therefore, it is good enough for engineering purposes. It is also seen from Figs. 7 and 8 that both methods encounter major problems: their error is much larger than the angular velocity to be measured. The question is now: "can anything more be done to make accelerometer strapdowns a viable solution for inertial navigation of UAVs?"

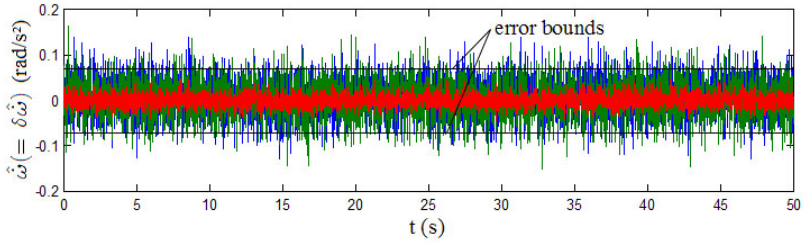

Figure 6: Estimated angular acceleration

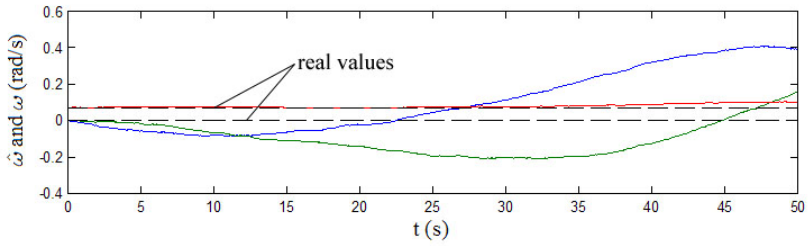

(a)

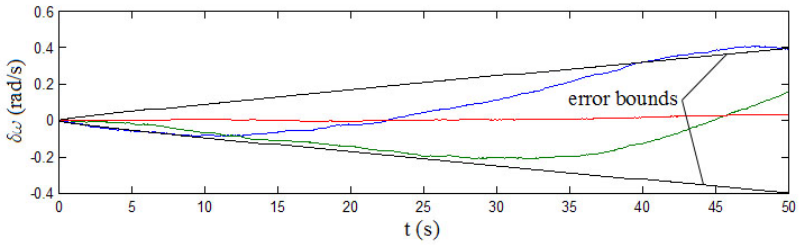

(b)

Figure 7: Angular velocity computed with the time-integration method: (a) estimates and (b) errors

One could propose to design a filter to reduce the noise level. Instead of doing this, let us simply remove the noise component from the accelerometer readouts to see if filtering has the potential of giving satisfying results. Keeping only the normally-distributed bias error $\delta a^b_{rms} = 0.1$ mg, we obtain the angular velocity estimates of Figs. 9 and 10. The time-integration method still yields bad results, with an error growth-rate of approximately 0.007 rad/s^2. On the other hand, the centripetal acceleration method gives more promising results: without noise, the estimates of the two null components of the angular velocity vanish. The error on the non-null component is approximately 0.01 rad/s$\approx 2000°$/h. This is still worse than most of low-cost angular-rate sensors. For example, the MEMS angular-rate sensors used by Brown and Lu (2003) have an accuracy of 500°/h. In fact, as the error bound is proportional to the bias in the accelerometers, it is apparent that a 25 μg accuracy is needed to obtain the same accuracy with an accelerometer strapdown.

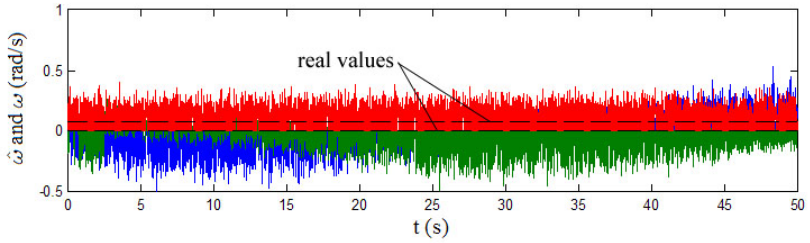

(a)

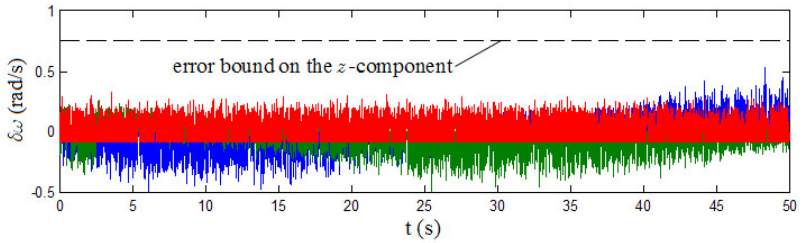

(b)

Figure 8: Angular velocity computed with the centripetal acceleration method: (a) estimates and (b) errors

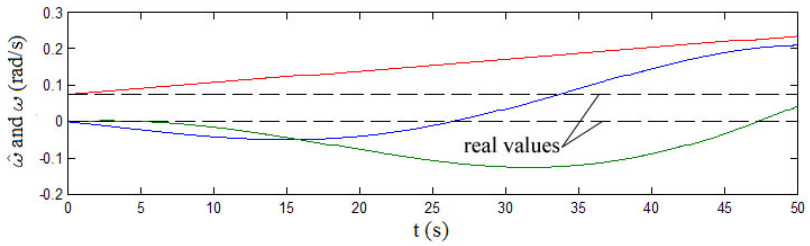

(a)

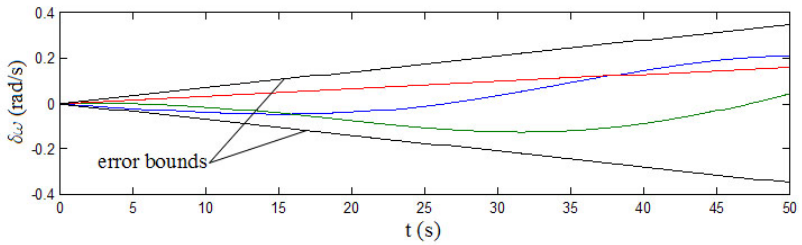

(b)

Figure 9: Angular velocity computed with the time-integration method from noiseless accelerometer readouts: (a) estimates and (b) errors

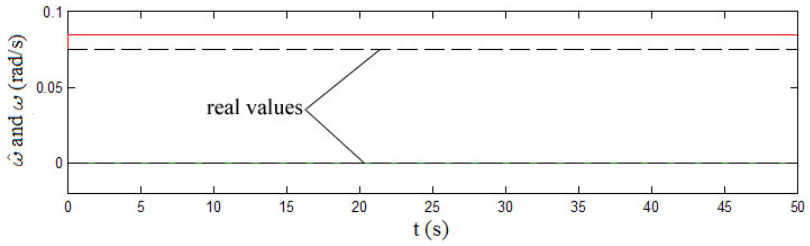

(a)

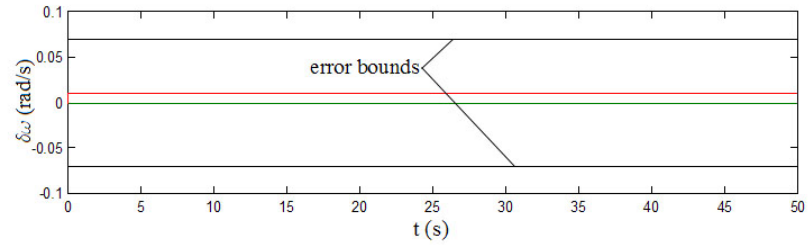

(b)

Figure 10: Angular velocity computed with the centripetal acceleration method from noiseless accelerometer read-outs: (a) estimates and (b) errors

6 CONCLUSIONS

The problem of estimating the angular velocity of a UAV was discussed in a general context, and, therefore, the resulting error analysis allows one to compare accelerometer strapdowns to strapdowns that are currently used in industry. The condition number of matrix $\overline{\mathbf{M}}$ was found to be an appropriate performance index to assess the quality of accelerometer strapdown geometries. As a result, the corresponding characteristic length represents the effective size of the accelerometer strapdown.

Provided that the strapdown geometry is known accurately, a safe error bound was found and validated for a stable estimate of the angular velocity—that is, using the centripetal acceleration method. This error bound is proportional to $\|\overline{\mathbf{M}}^{\dagger}\|_2$—which depends only on the strapdown geometry—to the errors in accelerometer readouts δa_{i1}, to $1/\left|\omega_i\right|$—where ω_i is the i^{th} component of the angular velocity—and to the inverse of the strapdown size l. Among these variables, the critical parameter is the error in the measurements, for the others are dictated by the UAV and its motion. The noise in the accelerometer signals can be reduced through filtering and sources of bias error can be identified and accounted for, but at what cost? From the foregoing error results, it does not seem worth the effort to replace angular-rate sensors with accelerometers, because the level of accuracy expected does not match the level of accuracy of expensive optical angular-rate sensors. In fact, in the case of a 1 m wingspan UAV and for the motion considered, the accelerometer strapdown could only approach the accuracy of low-cost angular-rate sensors, and this, under the ideal conditions of *perfect* noise filtering and with a bias error as low as 25 μg.

Nevertheless, accelerometer technology is still growing quickly and it may render all-accelerometer strapdowns a viable option for UAV INS in the near future. In this eventuality, the error formulas introduced here can be used to compare an all-accelerometer design with an angular-rate sensor design.

References

Analog Devices Industry, 2005, Data Sheets of ADXL203 Accelerometer, www.analog.com.

Angeles, J., 2003, *Fundamentals of Robotic Mechanical Systems*, Second Edition, Springer, New York, USA.

Bendat, J. S., Piersol, A. G., 1971, *Random Data: Analysis and Measurement Procedures*, John Wiley & Sons, New York, USA.

Brown, A. K., Lu, Y., 2003, "Performance Test Results of an Integrated GPS/MEMS Inertial Navigation Package", *NAVSYS Corporation.*

Golub, G. and Van Loan, C., 1983, *Matrix Computations*, Johns Hopkins University Press, Baltimore, USA.

Mostov, K. S., 2000, "Design of Accelerometer-Based Gyro-Free Navigation Systems", Ph.D. Dissertation, University of California, Berkeley, USA.

Padgaonkar, A. J., Krieger, K. W., and King, A. I., 1975, "Measurement of Angular Acceleration of a Rigid Body Using Linear Accelerometers", *ASME J. Applied Mechanics*, pp. 552–556.

Parsa, K., 2003, "Dynamics, State Estimation, and Control of Manipulators with Rigid and Flexible Subsystems", Ph.D. Dissertation, McGill University, Montreal, Canada.

Parsa, K., Angeles, J. and Misra, A. K., 2003, "Estimation of the Flexural States of a Macro-Micro Manipulator Using Accelerometer Data", *Proc. of the 2003 IEEE ICRA*, Taipei, Taiwan, Vol. 3, pp. 3120–3125.

Parsa, K., Angeles, J. and Misra, A. K., 2001, "Pose-and-Twist Estimation of a Rigid Body Using Accelerometers", *Proc. of the 2001 IEEE ICRA*, Seoul, Korea, Vol. 3, pp. 1873–1878.

Peng, Y. K., and Golnaraghi, M. F., 2004, "A vector-based gyro-free navigation system by integrating existing accelerometer network in an automobile", *Proc. of CSME Forum*, London, Canada, pp. 421–430.

Zorn, A. H., 2002, "GPS-Aided All-Accelerometer Inertial Navigation", *ION GPS 2002*, pp. 1442–1453.